



# Development and carotenoid synthesis in dark-grown carrot taproots require *PHYTOCHROME RAPIDLY REGULATED1*

Daniela Arias ,<sup>1</sup> Angélica Ortega ,<sup>1</sup> Christian González-Calquin,<sup>1</sup> Luis Felipe Quiroz ,<sup>1</sup> Jordi Moreno-Romero ,<sup>2,3</sup> Jaime F. Martínez-García<sup>2,3</sup> and Claudia Stange <sup>1,\*†</sup>

<sup>1</sup> Centro de Biología Molecular Vegetal, Facultad de Ciencias, Universidad de Chile, Santiago, Chile

<sup>2</sup> Centre for Research in Agricultural Genomics (CRAG), CSIC-IRTA-UAB-UB, Barcelona, Spain

<sup>3</sup> Institute for Plant Molecular and Cell Biology (IBMCP), CSIC-UPV, Universitat Politècnica de València, València, Spain

\*Author for correspondence: cstange@uchile.cl

†Senior author.

C.S. conceived the research plans. C.S. and J.F.M.G. supervised the experiments. D.A. and A.O. performed the experiments. J.M.R., C.G.C., and L.F.Q. performed some experiments with D.A. J.F.M.G. provided technical assistance to D.A. C.S. designed the experiments and analyzed the data. C.S. conceived the project and wrote the article with contributions of all the authors. C.S. agrees to serve as the author responsible for contact and ensures communication.

The author responsible for distribution of materials integral to the findings presented in this article in accordance with the policy described in the Instructions for Authors (<https://academic.oup.com/plphys/pages/general-instructions>) is: Claudia Stange (cstange@uchile.cl).

## Abstract

Light stimulates carotenoid synthesis in plants during photomorphogenesis through the expression of *PHYTOENE SYNTHASE* (*PSY*), a key gene in carotenoid biosynthesis. The orange carrot (*Daucus carota*) synthesizes and accumulates high amounts of carotenoids in the taproot that grows underground. Contrary to other organs, light impairs carrot taproot development and represses the expression of carotenogenic genes, such as *DcPSY1* and *DcPSY2*, reducing carotenoid accumulation. By means of RNA sequencing, in a previous analysis, we observed that carrot *PHYTOCHROME RAPIDLY REGULATED1* (*DcPAR1*) is more highly expressed in the underground grown taproot compared with those grown in light. *PAR1* is a transcriptional cofactor with a negative role in shade avoidance syndrome regulation in *Arabidopsis* (*Arabidopsis thaliana*) through the dimerization with *PHYTOCHROME-INTERACTING FACTORS* (*PIFs*), allowing a moderate synthesis of carotenoids. Here, we show that overexpressing *AtPAR1* in carrot increases carotenoid production in taproots grown underground as well as *DcPSY1* expression. The high expression of *AtPAR1* and *DcPAR1* led us to hypothesize a functional role of *DcPAR1* that was verified through *in vivo* binding to *AtPIF7* and overexpression in *Arabidopsis*, where *AtPSY* expression and carotenoid accumulation increased together with a photomorphogenic phenotype. Finally, *DcPAR1* antisense carrot lines presented a dramatic decrease in carotenoid levels and in relative expression of key carotenogenic genes as well as impaired taproot development. These results suggest that *DcPAR1* is a key factor for secondary root development and carotenoid synthesis in carrot taproot grown underground.

## Introduction

Light is an essential cue for plant development and growth since it is required for photosynthesis and photomorphogenesis (Tripathi et al., 2019). In both processes, the plastidial pigments chlorophylls and carotenoids fulfil crucial roles. Synthesis of chlorophylls and carotenoids is strongly promoted by light (Stange and Flores, 2012). Carotenoids also provide yellow, orange, and red colors to flowers, fruits, and some roots. These pigments are not only powerful antioxidant that protect plants from photooxidative damage but also precursors of important compounds such as the phytohormones strigolactones and abscisic acid (ABA) that affect plant development (Hirschberg, 2001; Howitt and Pogson, 2006; Sandmann et al., 2006; Rodríguez-Concepción, 2010; Ruyter-Spira et al., 2013; Sandmann, 2015; Simpson et al., 2016a). The first enzyme in carotenoid synthesis and the most regulated at the transcriptional and posttranscriptional level is phytoene synthase (PSY; Maass et al., 2009; Rodríguez-Villalón et al., 2009; Rosas-Saavedra and Stange, 2016). In *Arabidopsis* (*Arabidopsis thaliana*) this enzyme is encoded by the *AtPSY* gene, whereas in carrot (*Daucus carota*), it is encoded by two genes, *DcPSY1* and *DcPSY2* (Ruiz-Sola and Rodríguez-Concepción, 2012; Rodríguez-Concepción and Stange, 2013).

When seedlings germinate in the dark, they exhibit a pale yellow or rather whitish color due to the lack of pigmentation (etiolated seedlings). In these conditions, PHYTOCHROME-INTERACTING FACTORS (PIFs) accumulate and repress photomorphogenesis. PIFs are a subfamily of basic helix–loop–helix (bHLH) transcription factors that act as central mediators in a variety of light-mediated responses, including transitions from etiolated to photomorphogenic (de-etiolated) seedlings and plant responses to vegetation proximity (Leivar et al., 2009; Pham et al., 2018). As part of their repressive role of the photomorphogenic development in the dark, PIFs bind to *AtPSY* light-responsive elements (LREs, such as G-box), preventing *PSY* expression and impeding the synthesis and accumulation of carotenoids in these conditions (Toledo-Ortiz et al., 2010). Once the emerging seedlings perceive the light, photomorphogenesis is triggered, which results in inhibition of stem elongation (e.g. hypocotyls or epicotyls), promotion of cotyledon or/and leaf expansion, and promotion of chlorophyll and carotenoids synthesis, which result in the acquisition of the characteristic green color of plants (Quail, 2002; Kami et al., 2010; De Wit et al., 2016). Light perception is carried out by photoreceptors such as phytochromes (phys), cryptochromes, and phototropins (Kami et al., 2010; Stange and Flores, 2012; De Wit et al., 2016; Quian-Ulloa and Stange, 2021). In particular, phys participate in the induction of the expression of key carotenogenic genes such as *PSY* (Saijo et al., 2008; Stange and Flores, 2012; Chen et al., 2014; Bianchelli et al., 2018; Quian-Ulloa and Stange, 2021). During de-etiolation, the light activation of phys triggers PIF phosphorylation, which are subsequently degraded by the proteasome and/or inactivated, therefore making them unable to

bind to LREs (Bae and Choi, 2008; Shen et al., 2008; Shin et al., 2009; Toledo-Ortiz et al., 2010). This results in a rapid de-repression of *PSY* gene expression and a burst in the production of carotenoids in coordination with chlorophyll biosynthesis and chloroplast development for an optimal transition to photosynthetic metabolism (Toledo-Ortiz et al., 2010). In addition to repressing gene expression, PIFs also promote the expression of dozens of genes in the dark that are also rapidly downregulated after seedling de-etiolation, such as *A. thaliana* *PHYTOCHROME RAPIDLY REGULATED 1* (*AtPAR1*), that encodes a transcriptional cofactor of the bHLH family. *AtPAR1* physically interacts with PIFs and thereby prevents PIFs from binding to LREs found in promoters of photomorphogenic genes, thus producing an increase in carotenoids compared to plants grown in the dark (Bou-Torrent et al., 2015). Indeed, *A. thaliana* lines that overexpress *AtPAR1* present an increase in total carotenoids in photosynthetic tissues, an increase in *AtPSY* expression and an exacerbated photomorphogenic phenotype shown as a reduced hypocotyl length (Roig-Villanova et al., 2007; Hao et al., 2012; Zhou et al., 2014; Bou-Torrent et al., 2015).

Unlike other plants, orange carrots accumulate large amounts of carotenoids in underground and dark-grown taproots (Stange et al., 2008; Fuentes et al., 2012; Rodríguez-Concepción and Stange, 2013). Surprisingly, root exposure to white light (W) causes a reduction in the expression of carotenogenic genes such as *PSYs* and *LYCOPENE BETA-CYCLASES* (*LCYBs*) and a decrease in carotenoid levels (Fuentes et al., 2012; Llorente et al., 2017; Arias et al., 2020). Indeed, the carrot root grown in W has a thinner and greener phenotype and presents an enrichment of chloroplasts instead of carotenoid accumulating chromoplasts (Fuentes et al., 2012). The expression profile between carrot taproot grown in W and underground (dark-grown) was analyzed and compared through an RNA sequencing (RNA-seq) approach (Arias et al., 2020). This led us to identify several carrot genes related to photomorphogenesis, such as *DcPHYA*, *DcPHYB*, and *DcPAR1*, whose transcripts accumulated in the underground dark-grown taproot but rapidly decreased in the root when exposed to W (Arias et al., 2020).

In this work, we aimed to characterize the role of *DcPAR1* in carotenoid synthesis and development in carrot taproot. First, we showed that overexpression of *AtPAR1* in transgenic carrot leads to higher levels of carotenoids in taproots as well as higher *DcPSY1* expression suggesting a key role of *PAR1* in carrot carotenoid synthesis. The similarity of *AtPAR1* and *DcPAR1* led us to suggest a similar molecular role of *DcPAR1* as a bHLH member that was verified through the *in vivo* binding to the bHLH *AtPIF7* protein. In addition, in order to analyze if these two genes share functionality, that is, if they are orthologues, we determined the *DcPAR1* role in photomorphogenesis and in carotenoid synthesis by overexpressing it in *Arabidopsis*. We showed that overexpression of *AtPAR1* in transgenic carrot present higher levels of carotenoids in taproots as well as higher *DcPSY1* expression suggesting a key role of the *PAR1* in carrot

carotenoid synthesis. Most importantly, *DcPAR1* antisense carrot plants showed an impaired taproot development and a dramatic decrease in both carotenoid levels and in the relative expression of key carotenogenic genes. These results suggest that *DcPAR1* is a transcriptional cofactor with a key role in the regulation of taproot development and carotenoid synthesis in the carrot taproot grown underground.

## Results

### Carrot plants overexpressing *AtPAR1* present higher carotenoid levels and an increase in *DcPSY1* expression in the taproot grown underground

As a first approximation to determine *PAR1* function in carotenoid synthesis in the carrot taproot, we overexpressed *AtPAR1* in carrots. During carrot transformation it caught our attention that *AtPAR1* embryos presented an orange phenotype instead of the normal whitish coloration of wild-type (WT) embryos (Figure 1A). This early observation suggested that *AtPAR1* could promote the synthesis of carotenoids in carrots in early stages of development. Next, four

adult plants (grown 4 months in the greenhouse), that overexpressed *AtPAR1*, were selected, established as independent transgenic lines and subjected to molecular and biochemical analysis (Figure 1, B and C). Among the four lines, two of them presented higher levels of transgene relative expression in the taproot (OE1 and OE2; Figure 1B), which also showed an increase in *DcPSY1* expression relative to WT taproots (Figure 1B). On the contrary, *DcPSY2* showed a decrease in the relative expression (Figure 1B), whereas the endogenous *DcPAR1* was expressed at similar or reduced levels than WT plants (Supplemental Figure S1). Importantly, transgenic OE1 and OE2 lines, which have the highest expression levels of *AtPAR1* and *DcPSY1*, presented an average of 2.5 times more total carotenoids in their taproots ( $919.6 \mu\text{g g}^{-1}$  dry weight [DW] and  $796.1 \mu\text{g g}^{-1}$  DW of carotenoids, respectively) compared to WT plants ( $410.2 \mu\text{g g}^{-1}$  DW) (Figure 1C). Moreover, both OE1 and OE2 lines also present higher  $\beta$ -carotene level (2.3 and 2.4 times more than WT roots) and only the OE1 line has significantly higher levels of  $\alpha$ -carotene in their taproots (Figure 1C). These results

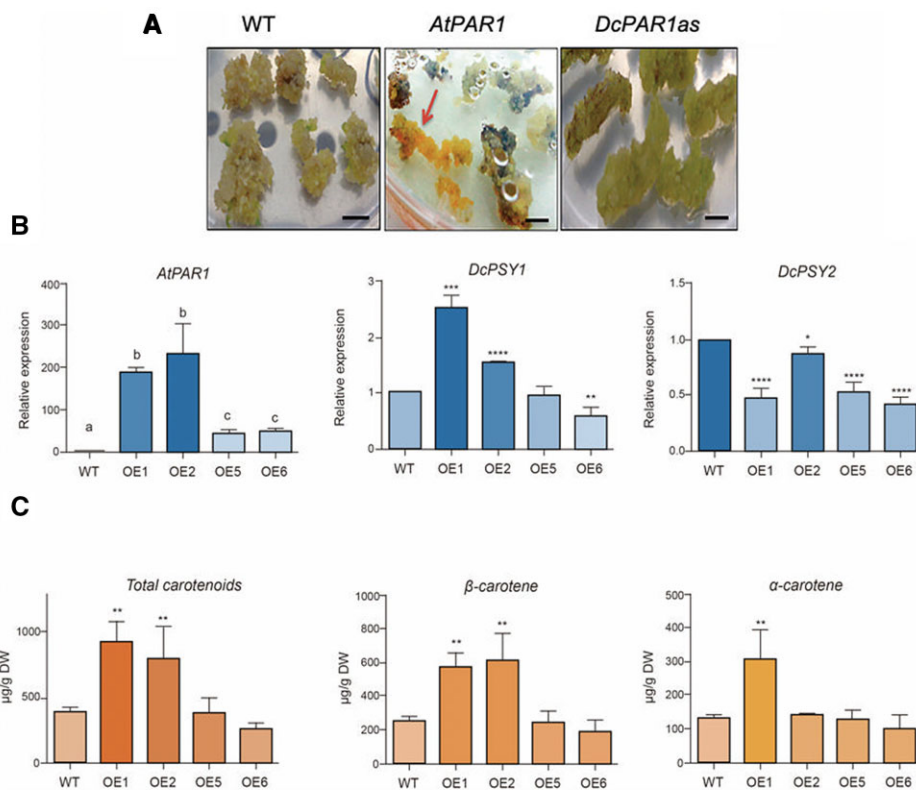


**Figure 1** Molecular and biochemical analysis of *AtPAR1* transgenic carrots. A, In vitro regeneration of carrot transformant plants. Embryo regeneration stage at 18–20 weeks after explants transformation is shown. The arrow indicates orange embryos that later give rise to whole carrot plants in *AtPAR1* (*AtPAR1*:GFP). WT, and *DcPAR1as* cream-colored embryos are also shown. Scale bar: 5 mm. B, Expression of *AtPAR1*, *DcPSY1*, and *DcPSY2* in transgenic (OE1, OE2, OE5, and OE6) and WT carrot taproots. Ubiquitin was used as housekeeping gene. The RT-qPCR was performed with three biological replicates (three different samples from the same transgenic lines) and two technical repeats each. C, Total carotenoids,  $\beta$ -carotene and  $\alpha$ -carotene levels in transgenic (OE1, OE2, OE5, and OE6) and WT carrot taproots. The analysis was repeated 3 times using three different samples from each transgenic line and three pools from three WT plants. Carotenoids are indicated in microgram per gram of DW. In (B) and (C) values are means  $\pm$  standard error (SE). Letters and asterisks indicate significant differences between WT and transgenic lines (one-way ANOVA analysis with Dunnett's post-hoc test; \*\*\*\* $P < 0.0001$ , \*\*\* $P < 0.001$ , \*\* $P < 0.01$ , \* $P < 0.1$ ).

suggest that *AtPAR1* positively regulates carotenoid synthesis by promoting the expression of the *DcPSY1*, but not *DcPSY2*.

### DcPAR1 interacts with AtPIF7 in the nucleus

The effect of *AtPAR1* overexpression on carrot taproot upon *DcPSY1* expression and carotenoid levels suggests that the product of a carrot *PAR1* homolog might have the same role as *AtPAR1* in *A. thaliana*. Therefore, we identified contig 42,760 (292 bp) obtained from the carrot transcriptome (Arias et al., 2020) which presented a 98% identity with *AtPAR1* (At2g42870, Access No NM\_129848.3) and obtained the CDS sequence of *DcPAR1* (Access No XM\_017390696.1) by searching in NCBI (Supplemental Figure S2). The complete CDS of *DcPAR1* (363 bp) presents a 57.7% nucleotide identity with the complete *AtPAR1* and 44% identity at the amino acid level (Figure 2A). We paid special attention to the bHLH domain considering that the *AtPAR1* protein presents a bHLH domain that allows it to interact with PIFs and with itself but not to DNA (Galstyan et al., 2011, 2012). A conserved domain search analysis was performed predicting a complete bHLH sequence between residues 29 and 107 (Figure 2A). Comparing this predicted sequence with *AtPAR1* bHLH, *DcPAR1* presented the key conserved Leu23 residue in Helix 1 (Figure 2B) and the conserved hydrophobic residues such as Val, Ala, Leu, and Ile in Helix 2, all of them important for dimer formation. In the basic domain, it presents an Asp, Glu, and Lys at positions 5, 9, and 13, respectively, that, similar to *AtPAR1* (Figure 2B), also differ from those (His5-Glu9-Arg13) required for DNA binding (Heim et al., 2003). This sequence analysis suggests that *DcPAR1* could be able to dimerize with other bHLH proteins but unable to bind DNA, functionally acting as a

transcriptional cofactor, as described for *AtPAR1* (Galstyan et al., 2011).

*AtPIF7* has been shown to bind to PHYB (Leivar et al., 2008) and to have a role in promoting Arabidopsis hypocotyls as a result of shade and warm temperature treatments (Li et al., 2012; Fiorucci et al., 2020). Considering that in *A. thaliana* a functional *AtPAR1* binds in vivo to PIFs and other bHLH proteins in the nucleus (Hao et al., 2012; Cifuentes-Esquivel et al., 2013; Paulišić et al., 2021), we aimed to determine whether the *DcPAR1* protein is nuclear and capable of heterodimerizing with other bHLH proteins. First, we observed that *DcPAR1*-GFP presents nuclear localization in cells of *Nicotiana benthamiana* leaves (Supplemental Figure S3). Next, we tested interaction of *DcPAR1* to *AtPIF7* in vivo in *N. benthamiana* cells by bimolecular fluorescence complementation (BiFC). In Figure 3, the reconstitution of YELLOW FLUORESCENCE PROTEIN (YFP) fluorescence is observed into the cell nucleus of leaves co-agroinfiltrated with the N-terminal part of the YFP, NY fused to *AtPIF7* (NY-*AtPIF7*) and the C-terminal part of the YFP (CY) fused to *DcPAR1* (CY-*DcPAR1*), thus demonstrating that both proteins interact in vivo. Fluorescence is also detected in NY-*DcPAR1* and CY-*DcPAR1* co-agroinfiltrations (Figure 3), indicating that *DcPAR1* can also homodimerize, as it was described for *AtPAR1* (Bou-Torrent et al., 2015). Together, these results suggested that *DcPAR1* has the ability to dimerize with itself and with PIFs, as it has been shown for *AtPAR1*.

### Arabidopsis plants that express *DcPAR1* present an increase in carotenoids with a higher *AtPSY* expression and *AtPSY* protein abundance

Taken in mind that overexpression of *AtPAR1* results in dwarf plants and increased *AtPSY* expression and carotenoid

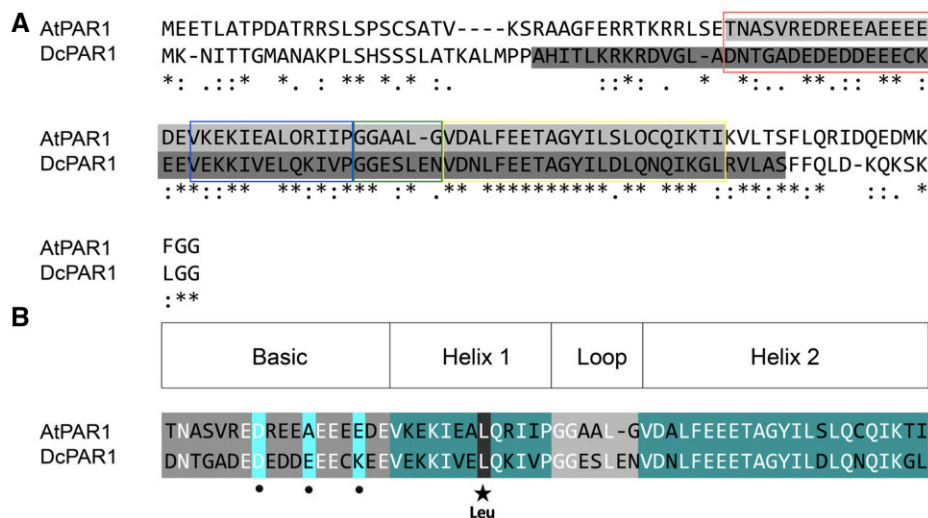


**Figure 2** *DcPAR1* and *AtPAR1* protein alignment. A, The predicted bHLH domains are highlighted in two shades of gray. The left box delimits the basic domain, while the next boxes mark the helix 1, the loop, and the helix 2 subdomains, respectively. B, Alignment of *AtPAR1* and *DcPAR1* bHLH domains. The subdomain extensions and conserved amino acids were described by Heim et al. (2003) and Roig-Villanova et al. (2007). Circles highlight residues 5, 9, and 13 (Asp, Ala, and Glu in *AtPAR1* and Asp, Glu, and Lys in *DcPAR1*). Star highlights the conserved leucine residue at position 23 in helix 1. Helix 2 shows hydrophobic residues, most of which are conserved in both proteins. Different and identical amino acids are highlighted in dark and white, respectively in each subdomain. All alignments were performed with Clustal Omega.

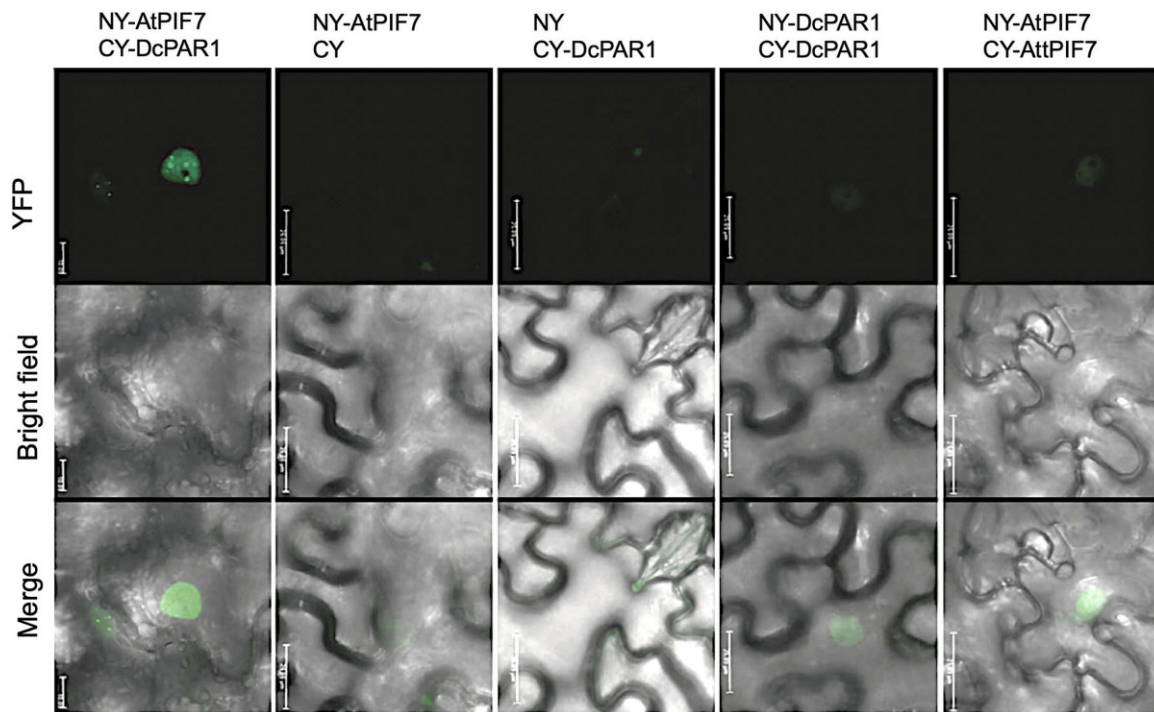


**Figure 3** Interaction in vivo between DcPAR1 and AtPIF7. BiFC assay between DcPAR1 and AtPIF7 is shown. The NY-AtPIF7/DcPAR1 corresponds to AtPIF7 or DcPAR1 genes cloned in fusion to N-terminal region of YFP (NY) gene and CY-AtPIF7/DcPAR1 corresponds to the same genes cloned in fusion to the CY. NY and CY are empty vectors. *Nicotiana benthamiana* leaves were co-infiltrated with the NY- and CY-derived plasmids to express the indicated fusion proteins. The top row shows the fluorescence of reconstituted YFP (indicative of a positive interaction of YN and YC fusions), the middle row shows the bright field of the same area and the bottom row shows the merge of previous conditions. Scale bar: 50  $\mu$ m.

level in Arabidopsis (Roig-Villanova et al., 2007; Bou-Torrent et al., 2015), we overexpressed DcPAR1 in Arabidopsis to evaluate if it provides similar phenotypes as AtPAR1. We obtained more than 20 independent transgenic lines and selected four T3 transgenic lines that express DcPAR1 (Figure 4A) for further analysis that was done in 2-week-old plants grown under W (long-day photoperiod). The relative expression of the endogenous AtPAR1 was not significantly affected in the transgenic lines except for L1, which presented a higher expression level than the WT line (Col-0; Figure 4A). Importantly, all transgenic lines presented a significant increase in AtPSY relative expression (Figure 4A), similar to AtPAR1 overexpressing lines (Bou-Torrent et al., 2015). The increase in the relative expression of AtPSY was accompanied by an increase in the abundance of PSY protein in all transgenic lines (Figure 4B; Supplemental Figure S4 shows Coomassie blue staining as control) and increased total carotenoids compared to Col-0 (Figure 4C), suggesting that DcPAR1 positively regulates the expression of AtPSY and thus increasing carotenoids content in Arabidopsis.

To determine if DcPAR1 also affects elongation, we performed phenotypic analysis in 2-week- and 1.5-month-old transgenic lines. In 2-week-old seedlings, transgenic lines presented a reduced length in hypocotyl, cotyledons, and primary leaves (Supplemental Figure S5) similar to that reported for Arabidopsis AtPAR1 overexpressing lines (Roig-Villanova et al., 2007; Hao et al., 2012; Zhou et al., 2014; Bou-Torrent et al., 2015). Moreover, all transgenic lines

present a dwarf phenotype (Figure 5A) with a significant reduced stem height and silique length (Figure 5B) at the mature stage. These results suggest that the DcPAR1 is functional in vivo in promoting carotenoid synthesis and inhibiting growth in *A. thaliana*.

### Repression of DcPAR1 expression affects carrot taproots growth, carotenoid composition, and carotenogenic gene expression

The next step was to evaluate the role of DcPAR1 in carrot. For this, transgenic antisense carrot plants for DcPAR1 were generated. During in vitro regeneration of DcPAR1 antisense (DcPAR1as) plants, no phenotypic differences were observed compared to WT embryogenesis (Figure 1A). Eleven mature plants were obtained, and the molecular analysis confirmed that ten of them were transgenic (Supplemental Figure S6). Four transgenic lines were selected for further molecular and biochemical analysis. As shown in Figure 6A, all transgenic lines presented an important reduction in DcPAR1 expression (between 80% and 99%) and a drastic reduction in the taproot secondary growth at the mature stage, as shown for line AS10 (Figure 6B). The taproots of a 4-month-old representative line that grew underground were considerably smaller and thinner than WT taproots of the same age and grown under the same conditions. The average mass of the transgenic roots did not exceed 400 mg while the average mass of a 4-month-old WT carrot taproot can weigh up to 7 g (Figure 6B). In addition, the roots were pale suggesting

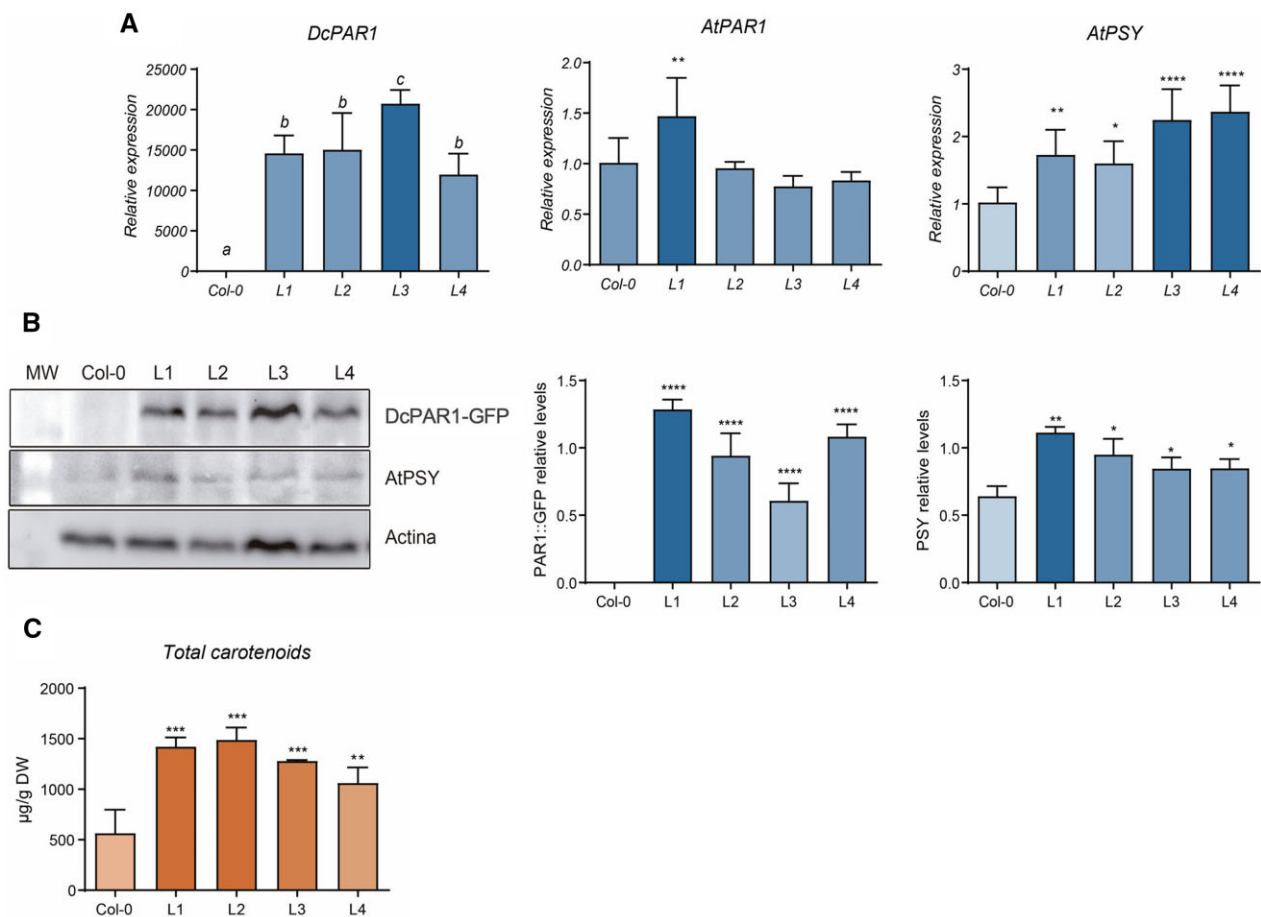


**Figure 4** Expression and carotenoid quantification of transgenic *Arabidopsis* lines overexpressing *DcPAR1*. **A**, Relative expression level of *DcPAR1*, *AtPAR1*, and *AtPSY* in 2-week-old 35S:*DcPAR1*-GFP (L1, L2, L3, and L4) transgenic lines. The relative expression levels were carried out with three biological replicates ( $n = 3$ ) and two technical repeats each and normalized to housekeeping gene *EF1A4*. Values are means  $\pm$  SE. **(B)** Immunoblot of *DcPAR1*-GFP, *AtPSY*, and actin in the transgenic *Arabidopsis* lines indicated in **(A)** using antiGFP, antiPSY, and anti-ACTIN antibodies. About 100  $\mu$ g of total protein corresponding to three plants was loaded in each lane. Graphs present the semi-quantification of *DcPAR1*-GFP and *AtPSY* from Immunoblot using actin abundance as normalizer. Each graph shows the average of three Immunoblots and values are means  $\pm$  SE. ImageJ program was used for WB semi quantification. MW, molecular weight; Col-0: WT plants; L1–L4, transgenic plants. **C**, Total carotenoid content in 2-week-old Col-0 and transgenic plants. Carotenoid quantification was carried out with two biological replicates ( $n = 3$ ) for each line. Values are means  $\pm$  SE. Concentration is presented in microgram per gram of DW. In **(A–C)**: asterisks indicate significant differences between WT and transgenic plants performed by one-way ANOVA analysis with Dunnett's post-hoc test; \*\*\*\* $P < 0.0001$ , \*\*\* $P < 0.001$ , \*\* $P < 0.01$ , \* $P < 0.1$ .

that a substantial reduction in carotenoid levels might have occurred (Figure 6B). In addition, expression of key genes required for carotenoid synthesis, *DcPSY1*, *DcPSY2*, *DcLCYE*, *DcLCYB2*, *DcCHXB1*, and *DcCHXB2*, was significantly lower in all silenced lines relative to the WT, showing a reduction between 40% and 99% (Figure 6C). Moreover, a 50%–80% decrease in total carotenoid levels in all silenced lines was also obtained (Figure 6D). Likewise, all the transgenic lines showed a 4- to 60-fold decrease in  $\alpha$ -carotene and 4- to 58-fold in  $\beta$ -carotene (Figure 6E). However, an unexpected 6- to 15-fold increase in lutein levels was obtained (Figure 6E). This pigment accumulates in photosynthetic tissues and in the WT carrot roots that grow exposed to light but not in the orange carrot taproot that grows underground (Fuentes et al., 2012).

In our experience, WT plants present a similar taproot phenotype and carotenoid content between three to

8 months of culture. With the purpose of verifying that the taproot phenotype in silenced plants persisted in time, plants were grown for four additional months (except the AS10 line that was harvested before and could not be recovered). We observed that, although the size of transgenic roots increased during the 4 months, they were still smaller and thinner than the WT taproots and presented a greenish coloration in the external part of the taproot and a yellowish coloration in the taproot center (Figure 7A). The relative expression level of *DcPAR1* in 8 months transgenic lines remained reduced between 60% and 75% (Figure 7A). Likewise, the relative expression of key carotenogenic genes in transgenic lines was still lower than in WT plants (Figure 7B), confirming that *DcPAR1* regulates the expression of carotenogenic genes in carrot root.

Carotenoids and chlorophylls quantification showed that *DcPAR1*as lines presented 2.4-fold fewer total carotenoids

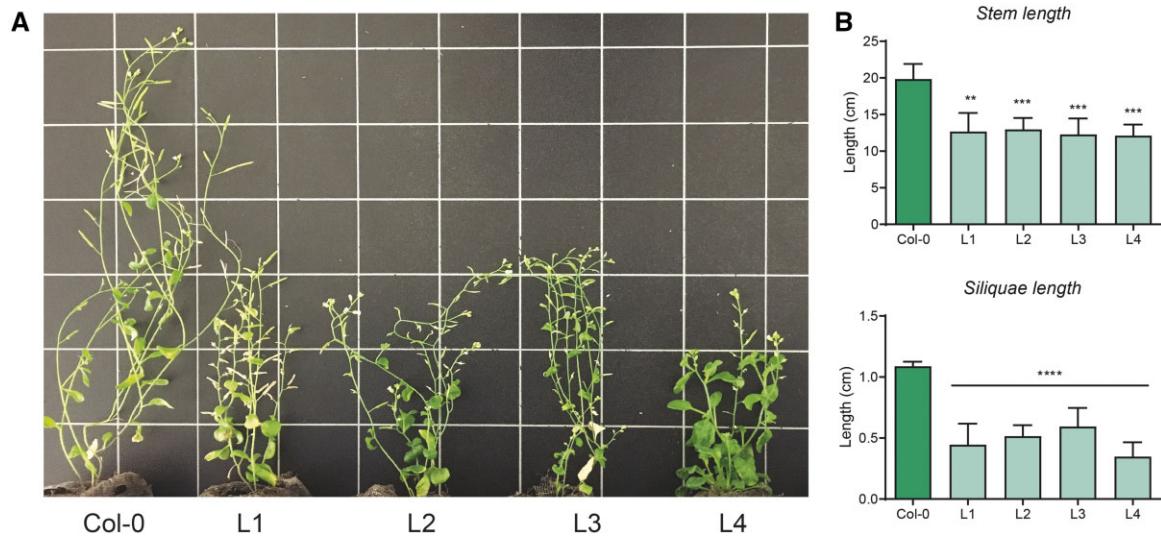


**Figure 5** Phenotype of mature transgenic *Arabidopsis* lines overexpressing *DcPAR1*. A, Picture showing the length and phenotype of representative 6-week-old plants of Col-0 and T3 transgenic lines. B, Stem and (C) Silique length of 6-week-old Col-0 and T3 transgenic plants. Each value is the mean  $\pm$  SE/SD of five plants each and using ImageJ program. Asterisks indicate significant differences between WT and transgenic plants performed by one-way ANOVA analysis with Dunnett's post-hoc test; \*\*\*\* $P < 0.0001$ , \*\*\* $P < 0.001$ , \*\* $P < 0.01$ , \* $P < 0.1$ .

(Figure 7C) and an increase of three- to five-fold to eight-fold in chlorophyll a and b reaching  $100\text{--}250\ \mu\text{g g}^{-1}$  DW (Figure 7D), suggesting that the absence of PAR1 leads to chloroplast instead of chromoplasts differentiation. Likewise, transgenic antisense plants presented a 3.5- to 14-fold reduction in  $\alpha$ -carotene and three- to nine-fold reduction in  $\beta$ -carotene levels with respect to WT plants. As in younger taproots, a significant increase in lutein was also observed, which reached up to  $200\text{--}250\ \mu\text{g g}^{-1}$  DW (compared to  $30\ \mu\text{g g}^{-1}$  DW in WT) (Figure 7E), thus explaining the yellowish coloration of antisense transgenic taproots with respect to the orange pigmentation of WT (Figure 7A). Taking all the results together, we suggest that *DcPAR1* is a functional cofactor that has an important regulatory role not only in carotenoid synthesis in carrot taproot that grows underground, but also in secondary taproot development.

## Discussion

### *DcPAR1* boosts carotenoid synthesis and promotes a photomorphogenic phenotype in *Arabidopsis*

Carotenoid biosynthesis regulation in plants has been extensively studied. Although there is much information about how this process is regulated by several factors, there is still much to explore with respect to how light regulates carotenoid biosynthesis in plant organs that normally grow with no direct W, such as roots (Stanley and Yuan, 2019; Quian-Ulloa and Stange, 2021). With the purpose to understand how carotenoids are synthesized in orange carrot taproot, we compared through RNA-seq the expression profile of carrot roots that grew in W with respect to those that grew underground (Arias et al., 2020). We identified several photomorphogenic genes that were upregulated in the underground condition and among them, *DcPAR1*, *DcPHYA*, and *DcPIF4* presented twice as much expression level in darkness

as in the root that grew in light (Arias et al., 2020). PAR1 is a recognized negative regulator of the shade avoidance syndrome (SAS) and a positive factor during seedling de-etioliation in *Arabidopsis* (Roig-Villanova et al., 2007; Hao et al., 2012; Zhou et al., 2014). In shade, the expression of *PAR1*, *PAR2*, and the *LONG HYPOCOTYL IN FAR RED 1* is induced, factors that encode transcriptional bHLH cofactors that participate in the compensation of excessive hypocotyl elongation during SAS (Roig-Villanova et al., 2007; Bou-Torrent et al., 2008; Hao et al., 2012; Zhou et al., 2014). From these factors, PAR1 interacts with several bHLH proteins that act as positive regulators of SAS such as BR-ENHANCED EXPRESSION (BEE), BES1-INTERACTING MYC-LIKE (BIM), and PIFs by partially preventing the binding of these transcription factors to LREs of photomorphogenic genes (Roig-Villanova et al., 2006, 2007; Hao et al., 2012; Cifuentes-Esquivel et al., 2013; Bou-Torrent et al., 2015; Ballaré and Pierik, 2017; Fernández-Milmanda and Ballaré, 2021; Quian-Ulloa and Stange, 2021). Importantly, PAR1 promotes *PSY* expression in leaves under shade (Bou-Torrent et al., 2015) and, of the positive SAS regulators BEEs, BIMs, and PIFs, only PIFs participate in repressing *PSY* expression and carotenoid synthesis in the shade (Toledo-Ortiz et al., 2010). PIFs remain stable in the shade condition and bind to the LRE motifs (Lorrain et al., 2008; Hornitschek et al., 2012). *Arabidopsis* RNAi-PAR1 and *par2* mutant lines have longer roots than WT. This suggest that AtPAR1, and its homolog AtPAR2 (Roig-Villanova et al., 2006, 2007), are active in roots and necessary for their correct development (Supplemental Figure S7).

AtPAR1 is a nuclear and atypical bHLH, it presents a functional HLH protein domain, but it lacks a functional DNA-binding domain, so its regulatory function is performed through the dimerization with PIFs transcription factors,

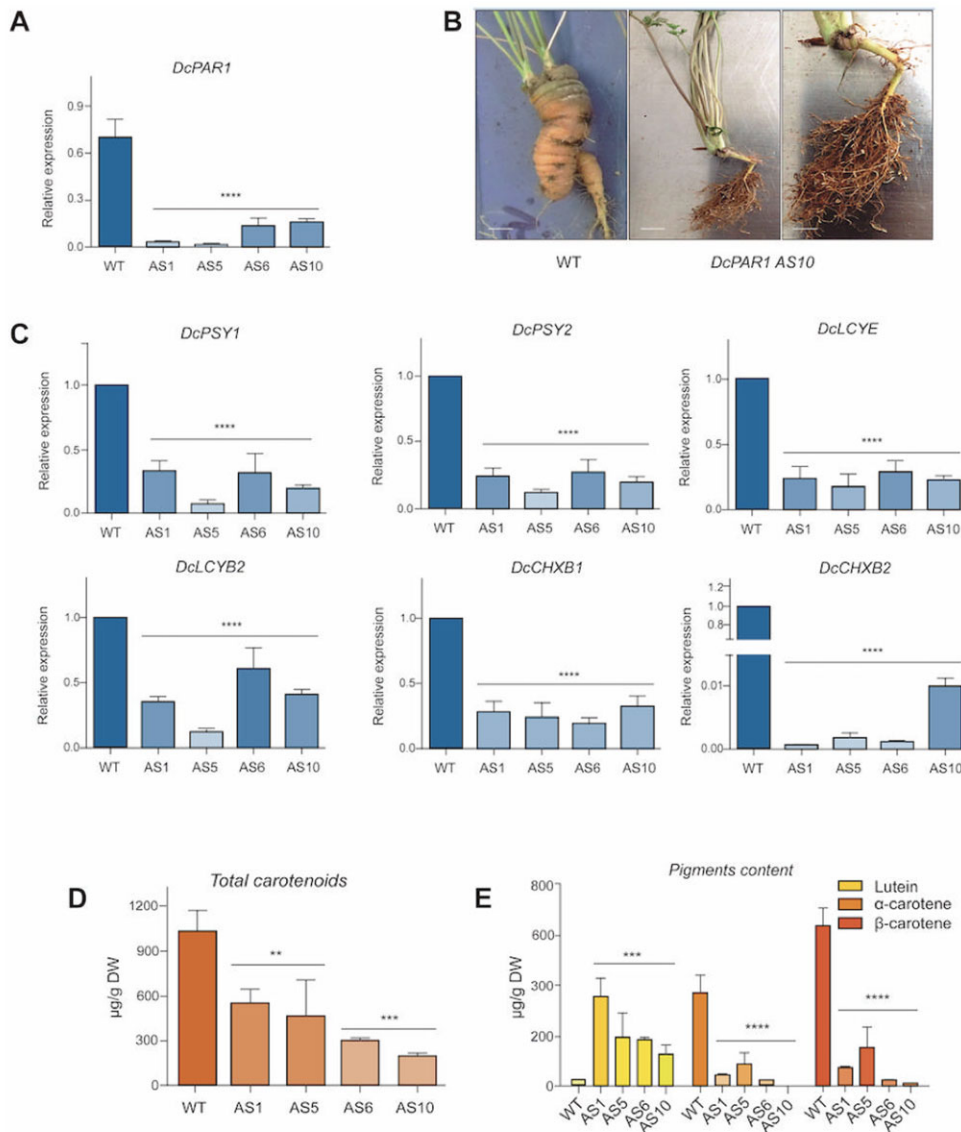


**Figure 6** Phenotype, expression analysis, and carotenoid content in 4-month-old DcPAR1as transgenic carrot taproots. A, Relative expression level of *DcPAR1* in AS1, AS5, AS6, and AS10 transgenic lines. The analysis was performed with three biological replicates (three different samples from the same transgenic lines) and two technical repeats each and normalized to the housekeeping *Ubiquitin* gene. WT was used as calibrator. B, Representative phenotype of a WT and a DcPAR1as transgenic carrot root (line AS10) grown 4 months underground after transplanting. Bar: 1 cm for left and center. Bar: 0.5 cm for the magnified version on the right. C, Relative expression level of *DcPSY1*, *DcPSY2*, *DcLCYE*, *DcLCYB2*, *DcCHXB1*, and *DcCHXB2*. The relative expression was carried out with three biological replicates (three different samples from the same transgenic lines) and two technical repeats each and normalized to the housekeeping *Ubiquitin* gene. WT was used as calibrator. D, Total carotenoids were quantified in a spectrophotometer at 474 nm and (E) lutein,  $\alpha$ -carotene, and  $\beta$ -carotene levels were determined by HPLC-DAD. Pigment content is indicated in microgram per gram of DW and was measured with three biological replicates (three different samples from the same transgenic lines). In (A) and (C–E): Values are means  $\pm$  SE. Asterisks indicate significant differences between transgenic lines and WT plant determined by one-way ANOVA analysis with Dunnett's post-hoc test; \*\*\*\* $P < 0.0001$ , \*\*\* $P < 0.001$ , \*\* $P < 0.01$ , \* $P < 0.1$ .

such as AtPIF4 and AtPIF1 (Roig-Villanova et al., 2007; Hao et al., 2012; Bou-Torrent et al., 2015).

Our bioinformatic analysis indicated that DcPAR1 has a similar structural pattern to AtPAR1, especially at the bHLH domain, suggesting that it could fulfill similar functions. Importantly, the key amino acids at the basic domain that determines the binding to DNA are also replaced by similar amino acids that are present in AtPAR1 (Heim et al., 2003;

Figure 2B). Likewise, the essential amino acids that determine the protein–protein interactions are still conserved in DcPAR1 (Heim et al., 2003; Figure 2B) which in functionality terms allows DcPAR1 to interact with other bHLH proteins, such as itself and AtPIF7 (Figure 3), an essential characteristic for a functional PAR1.

AtPAR1 interacts with AtPIF1, and consequently induces the expression of AtPSY, thus increasing the content of



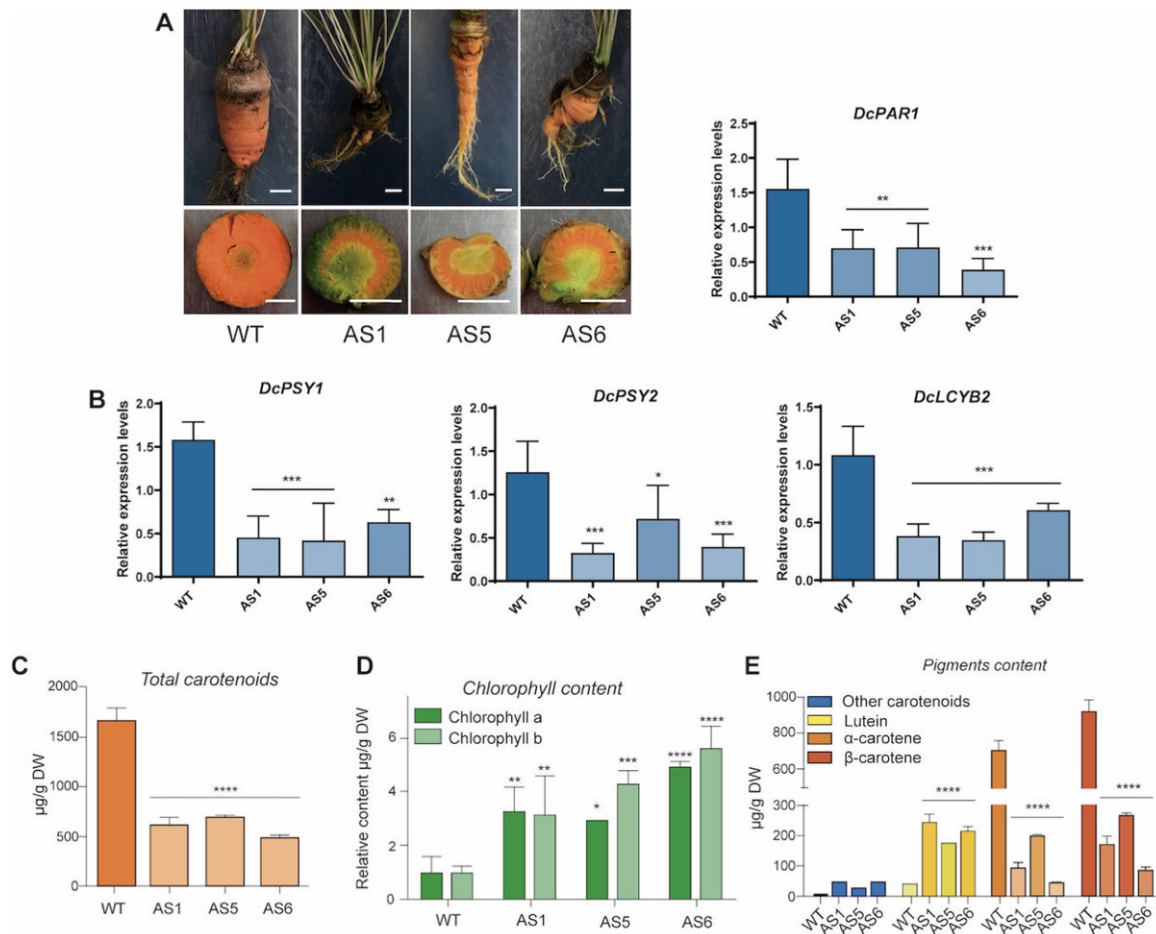


**Figure 7** Phenotype, expression analysis, and pigment content of 8-month-old DcPAR1as transgenic carrot taproots. A, Representative phenotype of carrot taproots of a WT and AS1, AS5, and AS6 DcPAR1as transgenic plants grown 8 months underground after transplanting (line AS10 was harvested at 4 months and not shown here). Bar: 1 cm. Graph in the right shows the relative expression level of *DcPAR1* in the indicated lines. Analysis was performed with three biological replicates (three different samples from the same transgenic lines) and two technical repeats each and normalized to the housekeeping *Ubiquitin* gene. B, Relative expression level of *DcPSY1*, *DcPSY2*, and *DcLCYB2*. Relative expression was carried out with three biological replicates (three different samples from the same transgenic lines) and two technical repeats each and normalized to the housekeeping *Ubiquitin* gene. C, Total carotenoids levels and (D) chlorophylls *a* and *b* in WT, AS1, AS5, and AS6 DcPAR1as carrot taproots. E, Lutein,  $\alpha$ -carotene, and  $\beta$ -carotene levels was determined by HPLC-DAD. Pigment content is indicated in microgram per gram of DW and was measured in triplicate, with three biological replicates (three different samples from the same transgenic lines). In (A–E): values are means  $\pm$  se. Asterisks indicate significant differences between transgenic lines and WT determined by one-way ANOVA analysis with Sidak post-hoc test; \*\*\*\* $P < 0.0001$ , \*\*\* $P < 0.001$ , \*\* $P < 0.01$ , \* $P < 0.1$ .

carotenoids together with the promotion of a photomorphogenic phenotype (Roig-Villanova et al., 2007; Bou-Torrent et al., 2015). Interestingly, Arabidopsis plants overexpressing *DcPAR1-GFP* and grown in W, presented a stable accumulation of DcPAR1-GFP, suggesting that it is stable in W, similarly to AtPAR1 that is stable in low and high R:FR, but not in the dark (Zhou et al., 2014). The higher DcPAR1-GFP accumulation correlates statistically with an increase in *AtPSY* relative expression levels and in PSY protein with a final rise in total carotenoids (Figure 4C), which strongly suggests a positive role of DcPAR1 on carotenoids synthesis in Arabidopsis. Indeed, the expression of the endogenous

AtPAR1 was not affected suggesting that PAR1 does not induce its own expression in Arabidopsis. It remains to be elucidated whether the DcPAR1 protein would be promoting *AtPSY* transcription through binding exclusively to PIF-type transcription factors or if there are other transcription factors that may be involved in this process, such as BEEs and BIMs (Cifuentes-Esquivel et al., 2013).

Moreover, according to the dwarf phenotype of Arabidopsis lines overexpressing *AtPAR1* (Roig-Villanova et al., 2007), 2-week-old *DcPAR1* transgenic lines presented several characteristics of a pronounced photomorphogenic phenotype (Supplemental Figure S5) that remains until

1.5 months (Figure 5). Given these results, we strongly suggest that *DcPAR1* and *AtPAR1* are orthologs.

### *DcPAR1* positively regulates carotenoid synthesis in carrot taproot

Considering that *AtPAR1* positively regulates the carotenoids synthesis in *Arabidopsis* photosynthetic tissue (Roig-Villanova et al., 2007; Bou-Torrent et al., 2015) we aimed to determine the *in vivo* role of *AtPAR1* in carotenoid synthesis in the carrot taproot.

Carrot *AtPAR1-GFP* lines with the highest transgene expression (OE1 and OE2) presented a significant increase in the relative expression levels of *DcPSY1*, but not in *DcPSY2* and *DcPAR1*, in a significant correlation with an increase in carotenoid levels in the taproot of mature carrots (Figure 1) but not in total carotenoid level in leaves (Supplemental Figure S8), suggesting that *AtPAR1:GFP* is sufficient and specific to increase carotenoid production in taproots. Interestingly, the transgenic lines with the lower transgene expression level (OE5 and OE6), produced a significant reduction in *DcPSY1* (except for OE5), *DcPSY2*, and *DcPAR1* expression but without affecting the level of carotenoids, which remains similar to the WT. The decrease in the relative expression of *DcPAR1* may be an endogenous compensation mechanism leading to speculate that *AtPAR1* may regulate the expression of its ortholog gene in carrot. Given these results, we suggest a positive regulation of *AtPAR1* on *DcPSY1* but not on *DcPSY2*, and that the effect generated is due to the expression of *AtPAR1* and not because of the endogenous gene.

The regulation of *AtPAR1* on the different *DcPSY* homologs may depend on the transcription factors that bind to their promoters that can be regulated by *AtPAR1*. It could be possible that *AtPAR1* dimerizes to some endogenous carrot PIFs that bind preferably to *DcPSY1* rather than to *DcPSY2* promoter, and the higher *AtPAR1* abundance may heterodimerize with and prevent this type of PIFs binding to *DcPSY1* promoter. Indeed, LREs are located in the *DcPSY1* and *DcPSY2* promoters (Simpson et al., 2018). It may be interesting to determine which transcription factors directly bind to the promoters of *DcPSY1* and *DcPSY2* in carrots. Since *DcPSY2* is mostly induced by salt stress and ABA and that AREB transcription factors are able to bind to *DcPSY2* promoter (Simpson et al., 2018), we suggest that *DcPSY2*, and not *DcPSY1*, is induced under abiotic stress (Simpson et al., 2018). It remains to be determined whether *DcPSY1* could be most associated to carotenoid synthesis during taproot development. On the other hand, in transgenic carrots that overexpress the *Arabidopsis* 1-deoxyxylulose-5-phosphate synthase (a gene that participates in the synthesis of the metabolic precursors for carotenoids) an increase in carotenoid levels was observed also with a significant correlation with an increase in the expression of *DcPSY1* and *DcPSY2* (Simpson et al., 2016b) suggesting that both genes determine the levels of carotenoids in carrot taproots.

The posttranscriptional gene silencing of *DcPAR1* in carrots is a better strategy to determine the role of the endogenous gene in carrots. *DcPAR1* antisense had important consequences on the carotenoid levels (Figures 6 and 7), which decrease significantly in correlation to a decrease in the expression of all carotenogenic genes analyzed, including both, *DcPSY1* and *DcPSY2* (Figures 6 and 7). Similar results were reported in *DcLCYB1* antisense carrots (Moreno et al., 2013), where a decrease of 40%–80% in total carotenoid levels together with a decrease in the expression levels of *DcPSY1* and *DcPSY2* was observed (Moreno et al., 2013). Moreover, *DcPAR1as* lines showed a dramatic reduction in the expression on all carotenogenic genes evaluated. Possibly, *DcPAR1* has the ability to bind to PIFs or other unknown transcription factors some of which would directly downregulate or upregulate *DcPSY1*, *DcPSY2*, *DcLCYB2*, *DcLCYE*, *DcCBHX1*, and/or *DcCBHX2*. It is also possible that *DcPAR1*–*DcPIFs* complex exerts a direct regulation upon *DcPSYs* and their activation has a direct impact on the other genes in the pathway. To establish a more in-depth explanation in this regard, it is necessary to determine which other factors, in addition to PIFs, are binding to *PAR1* in carrots during development and which transcription factors bind to promoters of carotenogenic genes, regulating their expression. In *Arabidopsis*, *ELONGATED HYPOCOTYL 5* (*HY5*) binds to PIFs and also competes with PIFs for binding to LRE, promoting *PSY* expression and inducing the differentiation of etioplasts into chloroplasts with increased carotenoids and chlorophylls in plants (Von Lintig et al., 1997; Ronen et al., 1999; Woitsch and Römer, 2003; Toledo-Ortiz et al., 2010). It has been proposed that there would be a genetic interaction between *AtPAR1* and *AtHY5* because double antisense-*PARs/hy5* mutants present a more elongated hypocotyl than simple mutants (Zhou et al., 2014). Therefore, *HY5* role in *PAR1* antisense lines could be explored. Nevertheless, these results support the hypothesis that *DcPAR1* would be a positive regulator of carotenoid synthesis in carrot taproot.

Carrot *DcPAR1as* lines produce a significant increase in lutein (in 4- and 8-month-old carrot taproots) similar to WT carrot roots grown in light, but absent in taproots grown underground (Fuentes et al., 2012; Arias et al., 2020). Most confusing is that *DcCHXB1* and *DcCHXB2* involved in lutein synthesis are deeply downregulated (Figure 6C), suggesting that the enzymes may be stabilized by an unknown mechanism.

In addition, 8-month-old *DcPAR1as* lines accumulate orange pigmented carotenoids in the phloem, while cortex and xylem display yellow/green pigmentation, a differential effect depending on the root tissue. Moreover, an increase in chlorophylls is also observed that are normally absent in WT taproots. These results suggest that *DcPAR1* is required for correct carotenoid synthesis. Indeed, *DcPAR1as* lines present chlorophylls similar than the WT roots that were grown in W (Fuentes et al., 2012) in which *DcPAR1*

expression is lower than that in the taproot grown underground (Arias et al., 2020).

### DcPAR1 positively regulates carrot taproot development

It has been shown that the accumulation of carotenoids in carrot roots is genetically associated with a homolog of the Arabidopsis *PSEUDO-ETIOLATION IN LIGHT* (*PEL*) gene (Iorizzo et al., 2016). *PEL* presumably acts as a repressor of photomorphogenesis. Carrot varieties with a loss-of-function allele of the *PEL* gene accumulate carotenoids in the root, suggesting that high pigment contents might result from a derepressed development of carotenoid-accumulating plastids (i.e. chloroplasts in the light but chromoplasts in the dark; Llorente et al., 2017). Our results support this possibility and go further in proposing DcPAR1 as an antagonistic factor of *PEL1*. Indeed, the expression of *AtPAR1* in carrots produces orange embryo showing an early and positive effect of PAR1 on carotenoid synthesis (Figure 1) but it did not generate an evident change in photomorphogenic phenotype at the mature stage.

Although *AtPAR1* antisense produced elongated and hyper-etiolated plants (Zhou et al., 2014), carrot DcPAR1as lines presented similar embryogenic and photomorphogenic development than control plants, although they presented up to 95% of *DcPAR1* reduced expression. However, the consequences in the taproot of DcPAR1as adult plants were drastic, showing a dramatic reduction in the size (thickness and length) and weight of the taproot in 4-month-old plants, a tendency that was maintained at 8 months of development. The phenotype obtained is partly reminiscent of that observed when silencing *DcLCYB1*, where the roots generated were thinner than the controls (Moreno et al., 2013) but less drastic than DcPAR1as, showing a relevant role for DcPAR1 in carrot taproot development.

Carrot root development has been previously reported to be closely related to carotenoid synthesis (Suslow et al., 1999; Cloutault et al., 2008). Thus, it is possible that both processes are being regulated by similar factors at the transcriptional or posttranscriptional level. PAR1 seems to be a good candidate to participate in both processes. These results and those reported in Arabidopsis suggest that PAR1 has an important regulatory role on carotenoid synthesis and development. Considering that PAR1 is upstream of the pigment synthesis pathway, it has a broader functional role on the carotenoid synthesis in parallel with the regulation of root development in the absence of W. *AtPAR1* reduces hypocotyl elongation in shade through the repression of auxin-induced genes such as the *SMALL AUXIN UP RNA15* (*SAUR15*) and *SAUR68* likely through their ability to inhibit DNA binding of PIFs or other bHLH to its binding motifs in the *SAUR15* and *SAUR68* promoters (Roig-Villanova et al., 2006, 2007; Bou-Torrent et al., 2008, 2015; Hao et al., 2012; Zhou et al., 2014). Moreover, some of the phenotypes of *AtPAR1* overexpressing lines are similar to those reported in auxin, brassinosteroid, or gibberellin mutants (Nakazawa

et al., 2001). Considering that DcPAR1as lines present a short and thin taproot with more lateral root abundance, we propose that DcPAR1 may promote auxin metabolism de-repression. Therefore, it remains unknown if DcPAR1 could have a role in hormone signaling during taproot development.

Based on our results, we propose a simple model regarding DcPAR1 role in carotenoid synthesis and taproot development (Figure 8). Exposure of the orange carrot roots to light (R/L) decreases *DcPAR1* transcripts levels in the nucleus, where PIFs are recruited and inactivated by PHYs, and competing with HY5 for binding to LRE, causing a low expression of carotenogenic genes such as *DcPSYs*. This leads to a reduced amount of PSY protein accumulation in plastids, which in turn generated a drop in total carotenoid accumulation with reduced  $\alpha$ -carotene and  $\beta$ -carotene levels but an increase in lutein and chlorophylls. This might result in chloroplast (rather than chromoplasts) differentiation and impairment in taproot development. On the contrary, in roots grown underground (e.g. covered with soil; R/D), the higher transcripts levels of *DcPAR1* may conduct to a higher recruitment and inactivation of PIFs, promoting an increased *DcPSYs* expression given by HY5.

As a consequence, high levels of PSY accumulate in plastids that lead to an increase in carotenoids synthesis (especially  $\alpha$ -carotene and  $\beta$ -carotene) that would promote chromoplast differentiation and secondary root development. Indeed, it was shown recently that synthetically inducing a burst in the production of phytoene (the product of the PSY enzymes and the first committed intermediate of the carotenoid pathway) elicits an artificial chloroplast-to-chromoplast differentiation in leaves (Llorente et al., 2020). Altogether, these results suggest that DcPAR1 is a key factor for secondary root development and carotenoid synthesis in carrot taproot grown underground.

## Conclusions

*DcPAR1*, like its Arabidopsis counterpart *AtPAR1*, induces *AtPSY* expression, boosts carotenoid synthesis, and produces a dwarf phenotype when overexpressed in *A. thaliana* while in carrot, *DcPAR1* positively regulates carotenoid synthesis and secondary root development in carrot taproot grown underground.

## Materials and methods

### Bioinformatic analysis

National Center for Biotechnology Information (NCBI) platform was used to obtain the complete CDS of *DcPAR1* using the contig 42,760 (202 bp) that corresponds to *DcPAR1* and was obtained from the RNA-seq analysis (Arias et al., 2020). Conserved domain search analysis was performed using the InterPro Scan (<https://www.ebi.ac.uk/interpro/search/sequence-search>) and SMART (<http://smart.embl-heidelberg.de/>) in order to identify the bHLH functional regions in *DcPAR1*. Sequence alignments were performed using Clustal Omega platform (<https://www.ebi.ac.uk/Tools/msa/clustalo/>).

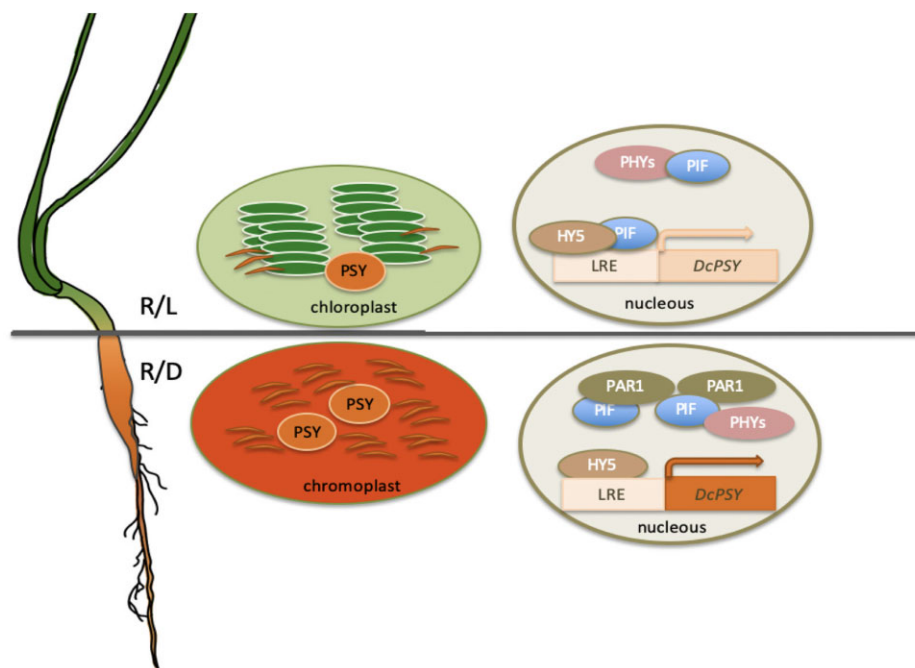


**Figure 8** Proposed model depicting the role of DcPAR1 in carrot taproot development and carotenoid synthesis. Roots grown exposed to W (R/L) present reduced expression of *DcPAR1* in the nucleus. We propose that PIFs are inactivated by PHYs and that HY5 competes with PIFs for binding to LRE, causing a low expression of carotenogenic genes such as *DcPSYs*. As a consequence, low level of PSY protein accumulates in plastids, producing reduced levels of total carotenoids,  $\alpha$ -carotene, and  $\beta$ -carotene accumulation but higher levels of chlorophylls and lutein, corresponding with chloroplast differentiation. Taproot development is also impaired. On the contrary, in the nucleus of roots grown underground (R/D), a high expression levels of *DcPAR1* takes place that permits a higher recruitment and inactivation of PIFs, promoting an increased *DcPSYs* expression given by HY5. Therefore, high levels of PSY accumulate in plastids leading to increased carotenoids synthesis corresponding with chromoplast differentiation and secondary taproot development.

### DcPAR1 gene amplification and vector construction

The complete CDS sequence of *PAR1* of carrot (*D. carota*) var. Nantaise (363 pb without stop codon) (NCBI access number XM\_017390696.1) was amplified from carrot taproot cDNA, using Herculase II Fusion DNA Polymerase (Agilent Technologies, Santa Clara, CA, USA) and DcPAR1.F and DcPAR1.R primers (Supplemental Table S1). The sequence was cloned into the entry PCR8/GW/TOPO vector (Invitrogen, Waltham, MA, USA) according to manufacturer's instructions and sequenced (Macrogen Corp., Rockville, MD, USA). Clones of PCR8:DcPAR1 in sense and antisense orientation were recombined with the destination vector pGWB5, obtaining the binary vectors pG5\_35S:PAR1:GFP (sense DcPAR1-GFP) and pG5\_35S:PAR1as (antisense DcPAR1as) that were used to overexpress and silence *DcPAR1*, respectively. The pBF1\_35S:AtPAR1-GFP binary vector was selected to overexpress *AtPAR1* as a fusion to the *GFP* reporter gene (AtPAR1-GFP) and has been described elsewhere (Roig-Villanova et al., 2007). All binary plasmids were transformed into *Agrobacterium tumefaciens* strain GV3101 for stable *Arabidopsis* (*A. thaliana*) and carrot transformation.

### Agrobacterium-mediated transformation of *D. carota* and *A. thaliana*

Commercial seeds of *D. carota* var. Nantaise were surface-sterilized and sown in culture medium Murashige and Skoog (MS; 4.4 g L<sup>-1</sup> MS salts; Murashige and Skoog, 1962, 20 g L<sup>-1</sup>

sucrose and 0.7% w/v agar) and grown in a culture chamber under 16-h long-day photoperiod at 23°C–25°C (W). Plants of 10- to 20-d postgermination were used for *Agrobacterium*-mediated transformation as described in Gonzalez-Calquin and Stange (2020). Briefly, the epicotyls of WT plants grown in vitro, were cut and co-cultivated in presence of *A. tumefaciens* strain GV3101 carrying the DcPAR1-GFP, DcPAR1as, or AtPAR1:GFP vectors and placed on solidified MS in darkness. After 2 d, the explants were transferred to MS culture medium supplemented with 1 mg L<sup>-1</sup> of 2,4-D, 50 mg L<sup>-1</sup> of Hygromycin (for transgene selection), and 200 mg L<sup>-1</sup> of Timentin (for *Agrobacterium* control) for embryo development. After 4–5 weeks in darkness, the explants were transferred to MS culture medium supplemented with 0.5 mg L<sup>-1</sup> of 2,4-D, 100 mg L<sup>-1</sup> of Hygromycin and 200 mg L<sup>-1</sup> of Timentin and grown in W (16-h long-day photoperiod at 23°C–25°C) for ~7 weeks. Finally, the hygromycin-resistant embryos were transferred to MS culture medium without hormones to promote elongation of carrot seedlings. Plants of 5–7 cm length were transferred to a mixture of soil: vermiculite (1:1) and maintained under the same photoperiod and temperature conditions described above. Transgenic plants were selected by amplifying the respective transgene form genomic DNA: *AtPAR1* gene in the case of carrot plants transformed with pBF1:AtPAR1:GFP (Bou-Torrent et al., 2015) with AtqPAR1.F and AtqPAR1.R

primers (Supplemental Table S1), *DcPAR1* gene in the case of *Arabidopsis* plants using primers DcqPAR1.F and DcqPAR1.R (Supplemental Table S1) or including *GFP* amplification in the case of carrot plants transformed with pG5:PAR1as, using primers DcPAR1.R and qEGFP.R (Supplemental Table S1).

*Arabidopsis thaliana* WT plants (Col-0 ecotype) were transformed using floral dip (Zhang et al., 2006). Seeds were surface sterilized in a solution of sodium hypochlorite (50% v/v) for 6 min, washed 3 times with sterile water and sown in solid MS medium (4.4 g L<sup>-1</sup> MS salts, 0.44% vitamins, 0.01% myo-inositol and 0.7% agar pH 5.8 with or without selection). They were kept in a growth chamber with a 16-h long-day photoperiod illuminated with cool-white fluorescent light (115- $\mu$ mol m<sup>-2</sup>s<sup>-1</sup>) at 22°C for 2–6 weeks depending on the experimental assay. Selected transgenic lines were transferred to a greenhouse in a mixture of soil:vermiculite (1:1) for molecular analysis. The selection of T3 homozygous transgenic lines was carried out by cultivation of selected transgenic T1, T2 and then T3 seeds in MS medium with hygromycin (15- $\mu$ g mL<sup>-1</sup>) and selected those T3 with up to 95% survival for further molecular, biochemical, and phenotypic analyses.

### Pigments extraction and quantification

In carrot and *Arabidopsis*, carotenoid and chlorophyll extraction was carried out as described previously (Simpson et al., 2016b). Pigments were extracted from 20 to 100 mg of fresh carrot transgenic taproots and 100 mg of entire 2-week-old *Arabidopsis* T3 lines with 4 mL of hexane:acetone:ethanol (2:1:1 v/v). After centrifugation, the upper phase was recovered and dried with N<sub>2</sub>. For total carotenoids and chlorophylls quantification, pigments were resuspended in 1 mL of acetone and quantified in a spectrophotometer (Shimadzu) at 750, 662, 645, and 474 nm in quartz cuvettes. Absorbance at 662, 645, and 474 nm permitted to determine the concentration of chlorophyll a, chlorophyll b, and total carotenoids, respectively. The absorbance at 750 nm determines the turbidity of the sample which may result in underestimation of the pigment concentration. Then, concentration of chlorophyll a, chlorophyll b and total carotenoids was determined as described previously (Lichtenthaler and Buschmann, 2001). Individual carotenoids were quantified in a Shimadzu HPLC (LC-10AT) with a diode array detector using a RP-18 Lichrocart 125-4 reverse phase column (Merck, Kenilworth, NJ, USA) and a mobile phase composed of acetonitrile:methanol:isopropanol (85:10:5 v/v). The separation of carotenoids and chlorophyll pigments was carried out with a 1.5 mL min<sup>-1</sup> flow rate, at room temperature, and under isocratic conditions. The identification of the pigments was performed as described by Simpson et al. (2016b).

### RNA extraction and RT-qPCR

RNA was obtained from 20 to 100 mg of fresh carrot tap roots or leaves and entire 2-week-old *Arabidopsis* plants that were pulverized with liquid nitrogen, homogenized

with CTAB buffer (2% (w/v) CTAB, 2% (w/v) PVP40, 25-mM ethylenediaminetetraacetic acid (EDTA), 2-M NaCl, 100-mM Tris-HCl (pH 8.0), and 0.05% spermidine trihydrochloride) and precipitated with LiCl (10 M) overnight. RNA was resuspended in nuclease-free water and the genomic DNA traces were eliminated by a 40 min DNase I treatment. For cDNA synthesis, 3  $\mu$ g of total RNA was incubated with 1 mM of Oligo-AP primer (Supplemental Table S1) and Improm II reverse transcriptase (Promega) according to the manufacturer's recommendations. Real time expression (RT-qPCR) was performed as described in Fuentes et al. (2012) and Moreno et al. (2013) in a Stratagene Mx3000P thermocycler, using SYBR Green double-strand DNA-binding dye. AtqPAR1.F and AtqPAR1.R primers were used to amplify a specific fragment of the coding sequences of *AtPAR1* (AT2G42870) and DcqPAR1.F and DcqPAR1.R for *DcPAR1* (XM\_017390696.1; Supplemental Table S1). DcqUbi.F and DcqUbi.R primers were used to amplify *Ubiquitin* and AtqPP2A.F and AtqPP2A.R to amplify *PP2A* housekeeping genes. Specific primers of carotenogenic genes *DcPSY1*, *DcPSY2*, *DcLCYB2*, *DcLCYE*, *DcCHXB1*, *DcCHXB2*, and *AtPSY* were the same as described in Fuentes et al. (2012) and summarized in Supplemental Table S1. The RT-qPCR analysis was performed with three biological replicates and two technical repeats and all reaction specificities were tested with melting gradient dissociation curves. To test for significant differences in gene expression, results were subjected to a one-way analysis of variance (ANOVA) ( $P < 0.05$ , confidence interval 95%) with Dunnett's post-hoc test according to the General Linear Models option in the statistical software package Graphpad Prism. The relative transcript levels were obtained using the Pfaffl equation (Pfaffl, 2001).

### BiFC assay

The PCR8:DcPAR1 vector was recombined with BiFC vectors (Gateway-based BiFC binary vectors, pYFC43 and pYFN43; Belda-Palaz3n et al., 2012), obtaining N-YFP:DcPAR1 and C-YFP:DcPAR1. The BiFC binary vectors (Belda-Palaz3n et al., 2012) and N-YFP:AtPIF7 and C-YFP:AtPIF7 vectors were provided by Dr Jaume Mart3nez-Garc3a (IBMCP CSIC-UPV, Valencia, Spain). The four vectors were transformed in *Agrobacterium* GV3101 and used for *N. benthamiana* agroinfiltration (Simpson et al., 2018). Four days after injection, YFP fluorescence was detected under a LEICA TCS SP5 confocal microscope with a light excitation wavelength of 488 nm and a filter for YFP at 520–560 nm. The images were obtained and processed with Leica LAS AF Lite software.

### Arabidopsis protein extraction and western blot

The *Arabidopsis* protein extraction was performed according to Saucedo et al. (2019) with modifications. Briefly, 400 mg of fresh tissue of entire 2-week-old *Arabidopsis* plants were pulverized with liquid nitrogen and then 4 mL of extraction buffer [0.5 M Tris-HCl pH 8, 0.7 M Sucrose, 2 protease inhibitor tablets (complete Mini, EDTA-free-Thermo Scientific Lot # UG27666820), 50-mM EDTA, KCl 0.1 M,  $\beta$ -mercaptoethanol 0.2%] were added and homogenized until the sample

was completely thawed. Then, 2 mL of basic saturated phenol pH 8.0 (Winkler, Hackensack, NJ, USA; # 20192088) were added, shaken 10 min in ice, and centrifuged at 8,000 g for 19 min at 4°C. The supernatant was recovered and four volumes of 0.1-M ammonium acetate in methanol (Merck gradient for liquid chromatography) were added, and proteins were precipitate overnight at -20°C. After centrifugation, the pellet was washed with 0.1-M ammonium acetate in methanol, and with acetone. The remaining acetone was evaporated at room temperature and the proteins (pellet) were stored at -20°C in resuspension buffer (100-mM Tris-HCl pH 7.0, 1% SDS). The extraction was carried out in triplicate for each transgenic line and control.

### Accession numbers

Sequence data from this article can be found in the GenBank/EMBL data libraries under the accession numbers indicated in Supplemental Figure S2.

### Supplemental data

The following materials are available in the online version of this article.

**Supplemental Table S1.** Primers used in this work.

**Supplemental Figure S1.** Expression of *DcPAR1* in carrot lines overexpressing *AtPAR1*.

**Supplemental Figure S2.** Sequences of contig 42.760 (Arias et al., 2020) and complete CDS of the *DcPAR1* gene (access number XM\_017390696.1).

**Supplemental Figure S3.** Subcellular localization of *DcPAR1:GFP*.

**Supplemental Figure S4.** Sodium dodecyl sulfate–polyacrylamide gel electrophoresis (SDS–PAGE) of *Arabidopsis DcPAR1* transgenic lines.

**Supplemental Figure S5.** Phenotypic analysis of 2-week-old *Arabidopsis* transgenic lines that overexpress *DcPAR1*.

**Supplemental Figure S6.** Transgenic selection of *DcPAR1as* carrot lines.

**Supplemental Figure S7.** Root length of *Arabidopsis* seedlings with reduced levels in *AtPAR1* and *AtPAR2*.

**Supplemental Figure S8.** Total carotenoids in leaves of carrot lines overexpressing *AtPAR1*.

### Funding

This study was supported by Chilean ANID Fondecyt Grant 1180747 (C.S.), MCIN/AEI/10.13039/501100011033/ and “ERDF A way of making Europe” grant BIO2017-85316-R and MCIN/AEI/10.13039/501100011033 grant PID2020-115782GB-I00 to J.F.M.G., European Commission contract H2020-MCSAIF-2017 (proposal 797473) to J.M.R.

*Conflict of interest statement.* All authors declare that they do not have conflict of interest.

### References

Arias D, Maldonado J, Silva H, Stange C (2020) A de novo transcriptome analysis revealed that photomorphogenic genes are

required for carotenoid synthesis in the dark-grown carrot taproot. *Mol Genet Genomics* **295**: 1379–1392

Bae G, Choi G (2008) Decoding of light signals by plant phytochromes and their interacting proteins. *Annu Rev Plant Biol* **59**: 281–311

Ballaré CL, Pierik R (2017) The shade-avoidance syndrome: multiple signals and ecological consequences. *Plant Cell Environ* **40**: 2530–2543

Belda-Palazón B, Ruiz L, Martí E, Tárraga S, Tiburcio AF, Culiáñez F, Farrás R, Carrasco P, Ferrando A (2012) Aminopropyltransferases involved in polyamine biosynthesis localize preferentially in the nucleus of plant cells. *PLoS One* **7**: e46907

Bianchetti ER, Silvestre Lira B, Santos Monteiro S, Demarco D, Purgatto E, Rothan C, Rossi M, Freschi L (2018) Fruit-localized phytochromes regulate plastid biogenesis, starch synthesis, and carotenoid metabolism in tomato. *J Exp Bot* **69**: 3573–3586

Bou-Torrent J, Roig-Villanova I, Galstyan A, Martínez-García JF (2008) PAR1 and PAR2 integrate shade and hormone transcriptional networks. *Plant Signal Behav* **3**: 453–454

Bou-Torrent J, Toledo-Ortiz G, Ortiz-Alcaide M, Cifuentes-Esquivel N, Halliday KJ, Martínez-García JF, Rodríguez-Concepcion M (2015) Regulation of carotenoid biosynthesis by shade relies on specific subsets of antagonistic transcription factors and cofactors. *Plant Physiol* **169**: 1584–1594

Chen F, Li B, Li G, Charron JB, Dai M, Shi X, Deng XW (2014) *Arabidopsis* phytochrome a directly targets numerous promoters for individualized modulation of genes in a wide range of pathways. *Plant Cell* **26**: 1949–1966

Cifuentes-Esquivel N, Bou-Torrent J, Galstyan A, Gallemí M, Sessa G, Salla Martret M, Roig-Villanova I, Ruberti I, Martínez-García JF (2013) The bHLH proteins BEE and BIM positively modulate the shade avoidance syndrome in *Arabidopsis* seedlings. *Plant J* **75**: 989–1002

Cloutault J, Peltier D, Berruyer R, Thomas M, Briard M, Geoffriau E (2008) Expression of carotenoid biosynthesis genes during carrot root development. *J Exp Bot* **59**: 3563–3573

De Wit M, Galvão VC, Fankhauser C (2016) Light-mediated hormonal regulation of plant growth and development. *Annu Rev Plant Biol* **67**: 513–537

Fernández-Milmanda GL, Ballaré CL (2021) Shade avoidance: expanding the color and hormone palette. *Trends Plant Sci* **26**: 509–523

Fiorucci AS, Galvão VC, Ince YÇ, Boccaccini A, Goyal A, Allenbach Petrolati L, Trevisan M, Fankhauser C (2020) PHYTOCHROME INTERACTING FACTOR 7 is important for early responses to elevated temperature in *Arabidopsis* seedlings. *New Phytol* **226**: 50–58

Fuentes P, Pizarro L, Moreno JC, Handford M, Rodríguez-Concepcion M, Stange C (2012) Light-dependent changes in plastid differentiation influence carotenoid gene expression and accumulation in carrot roots. *Plant Mol Biol* **79**: 47–59

Galstyan A, Bou-Torrent J, Roig-Villanova I, Martínez-García JF (2012) A dual mechanism controls nuclear localization in the atypical basic-helix-loop-helix protein PAR1 of *Arabidopsis thaliana*. *Mol Plant* **5**: 669–677

Galstyan A, Cifuentes-Esquivel N, Bou-Torrent J, Martínez-García JF (2011) The shade avoidance syndrome in *Arabidopsis*: a fundamental role for atypical basic helix-loop-helix proteins as transcriptional cofactors. *Plant J* **66**: 258–267

Gonzalez-Calquín C, Stange C (2020) *Agrobacterium tumefaciens*-mediated stable transformation of *Daucus carota*. *Methods Mol Biol* **2083**: 313–320

Hao Y, Oh E, Choi G, Liang Z, Wang ZY (2012) Interactions between HLH and bHLH factors modulate light-regulated plant development. *Mol Plant* **5**: 688–697

Heim MA, Jakoby M, Werber M, Martin C, Weishaar B, Bailey PC (2003) The basic helix-loop-helix transcription factor family in

- plants: a genome-wide study of protein structure and functional diversity. *Mol Biol Evol* **20**: 735–747
- Hirschberg J** (2001) Carotenoid biosynthesis in flowering plants. *Curr Opin Plant Biol* **4**: 210–218
- Hornitschek P, Kohnen MV, Lorrain S, Rougemont J, Ljung K, López-Vidriero I, Franco-Zorrilla JM, Solano R, Trevisan M, Pradervand S, et al.** (2012) Phytochrome interacting factors 4 and 5 control seedling growth in changing light conditions by directly controlling auxin signaling. *Plant J* **71**: 699–711
- Howitt CA, Pogson BJ** (2006) Carotenoid accumulation and function in seeds and non-green tissues. *Plant Cell Environ* **29**: 435–445
- Iorizzo M, Ellison S, Senalik D, Zeng P, Satapoomin P, Huang J, Bowman M, Iovene M, Sanseverino W, Cavagnaro P, et al.** (2016) A high-quality carrot genome assembly provides new insights into carotenoid accumulation and asterid genome evolution. *Nat Genet* **48**: 657–666
- Kami C, Lorrain S, Hornitschek P, Fankhauser C** (2010) Light-regulated plant growth and development. *Curr Top Dev Biol* **91**: 29–66
- Leivar P, Monte E, Oka Y, Liu T, Carle C, Castillon A, Huq E, Quail PH** (2008) Multiple phytochrome-interacting bHLH transcription factors repress premature seedling photomorphogenesis in darkness. *Curr Biol* **18**: 1815–1823
- Leivar P, Tepperman JM, Monte E, Calderon RH, Liu TL, Quail PH** (2009) Definition of early transcriptional circuitry involved in light-induced reversal of PIF-imposed repression of photomorphogenesis in young *Arabidopsis* seedlings. *Plant Cell* **21**: 3535–3553
- Li L, Ljung K, Breton G, Schmitz RJ, Pruneda-Paz J, Cowing-Zitron C, Cole BJ, Ivans LJ, Pedmale UV, Jung HS, et al.** (2012) Linking photoreceptor excitation to changes in plant architecture. *Genes Dev* **26**: 785–790
- Lichtenthaler HK, Buschmann C** (2001) Extraction of photosynthetic tissues: chlorophylls and carotenoids. *Current Protocols in Food Analytical Chemistry*, Vol. 1. John Wiley, Hoboken, NJ
- Llorente B, Martínez-García JF, Stange C, Rodríguez-Concepción M** (2017) Illuminating colors: regulation of carotenoid biosynthesis and accumulation by light. *Curr Opin Plant Biol* **37**: 49–55
- Llorente B, Torres-Montilla S, Morelli L, Florez-Sarasa I, Matus JT, Ezquerro M, D'Andrea L, Troncoso A, Majer E, Picó B, et al.** (2020) Synthetic conversion of leaf chloroplasts into carotenoid-rich plastids reveals mechanistic basis of natural chloroplast development. *Proc Natl Acad Sci USA* **117**: 21796–21803
- Lorrain S, Allen T, Duek PD, Whitelam GC, Fankhauser C** (2008) Phytochrome-mediated inhibition of shade avoidance involves degradation of growth-promoting bHLH transcription factors. *Plant J* **53**: 312–323
- Maass D, Arango J, Wüst F, Beyer P, Welsch R** (2009) Carotenoid crystal formation in *Arabidopsis* and carrot roots caused by increased phytoene synthase protein levels. *PLoS One* **4**: e6373
- Moreno JC, Pizarro L, Fuentes P, Handford M, Cifuentes V, Stange C** (2013) Levels of lycopene  $\beta$ -cyclase 1 modulate carotenoid gene expression and accumulation in *Daucus carota*. *PLoS One* **8**: e58144
- Murashige T, Skoog F** (1962) A revised medium for rapid growth and bio assays with tobacco tissue cultures. *Plant Physiol* **15**: 473–497
- Nakazawa M, Yabe N, Ichikawa T, Yamamoto YY, Yoshizumi T, Hasunuma K, Matsui M** (2001) DFL1, an auxin-responsive GH3 gene homologue, negatively regulates shoot cell elongation and lateral root formation, and positively regulates the light response of hypocotyl length. *Plant J* **25**: 213–221
- Paulišić S, Qin W, Arora Verasztó H, Then C, Alary B, Nogue F, Tsiantis M, Hothorn M, Martínez-García JF** (2021). Adjustment of the PIF7-HFR1 transcriptional module activity controls plant shade adaptation. *EMBO J* **40**: e104273
- Pfaffl MW** (2001) A new mathematical model for relative quantification in real-time RT-PCR. *Nucleic Acids Res* **29**: e45
- Pham VN, Kathare PK, Huq E** (2018) Phytochromes and phytochrome interacting factors. *Plant Physiol* **176**: 1025–1038
- Quail PH** (2002) Phytochrome photosensory signalling networks. *Nat Rev Mol Cell Biol* **3**: 85–93
- Quián-Ulloa R, Stange C** (2021) Carotenoid biosynthesis and plastid development in plants: the role of light. *Int J Mol Sci* **22**: 1184
- Rodríguez-Concepción M** (2010) Supply of precursors for carotenoid biosynthesis in plants. *Arch Biochem Biophys* **504**: 118–122
- Rodríguez-Concepción M, Stange C** (2013) Biosynthesis of carotenoids in carrot: an underground story comes to light. *Arch Biochem Biophys* **539**: 110–116.
- Rodríguez-Villalón A, Gas E, Rodríguez-Concepción M** (2009) Phytoene synthase activity controls the biosynthesis of carotenoids and the supply of their metabolic precursors in dark-grown *Arabidopsis* seedlings. *Plant J* **60**: 424–435
- Roig-Villanova I, Bou-Torrent J, Galstyan A, Carretero-Paulet L, Portolés S, Rodríguez-Concepción M, Martínez-García JF** (2007) Interaction of shade avoidance and auxin responses: a role for two novel atypical bHLH proteins. *EMBO J* **26**: 4756–4767
- Roig-Villanova I, Bou J, Sorin C, Devlin PF, Martínez-García JF** (2006) Identification of primary target genes of phytochrome signaling. Early transcriptional control during shade avoidance responses in *Arabidopsis*. *Plant Physiol* **141**: 85–96
- Ronen G, Cohen M, Zamir D, Hirschberg J** (1999) Regulation of carotenoid biosynthesis during tomato fruit development: expression of the gene for lycopene epsilon-cyclase is down-regulated during ripening and is elevated in the mutant Delta. *Plant J* **17**: 341–351
- Rosas-Saavedra C, Stange C** (2016) Biosynthesis of carotenoids in plants: enzymes and color. *Subcell Biochem* **79**: 35–69
- Ruiz-Sola MÁ, Rodríguez-Concepción M** (2012) Carotenoid biosynthesis in *Arabidopsis*: a colorful pathway. *Arabidopsis Book* **10**: e0158
- Ruyter-Spira C, Al-Babili S, Krol S, Bouwmeester H** (2013) The biology of strigolactones. *Trends Plant Sci* **18**: 72–83
- Saijo Y, Zhu D, Li J, Rubio V, Zhou Z, Shen Y, Hoecker U, Wang H, Deng XW** (2008) *Arabidopsis* COP1/SPA1 complex and FHY1/FHY3 associate with distinct phosphorylated forms of phytochrome A in balancing light signaling. *Mol Cell* **31**: 607–613
- Sandmann G** (2015) Carotenoids of biotechnological importance. *Adv Biochem Eng Biotechnol* **148**: 449–467
- Sandmann G, Römer S, Fraser PD** (2006) Understanding carotenoid metabolism as a necessity for genetic engineering of crop plants. *Metab Eng* **8**: 291–302
- Saucedo S, González A, Gómez M, Contreras RA, Laporte D, Sáez CA, Zúñiga G, Moenne A** (2019) Oligo-carrageenan kappa increases glucose, trehalose and TOR-P and subsequently stimulates the expression of genes involved in photosynthesis, and basal and secondary metabolisms in *Eucalyptus globulus*. *BMC Plant Biol*. **19**: 258
- Shen H, Zhu L, Castillon A, Majee M, Downie B, Huq E** (2008) Light-induced phosphorylation and degradation of the negative regulator phytochrome-interacting factor1 from *Arabidopsis* depend upon its direct physical interactions with photoactivated phytochromes. *Plant Cell* **20**: 1586–1602
- Shin J, Kim K, Kang H, Zulfugarov IS, Bae G, Lee CH, Lee D, Choi G** (2009) Phytochromes promote seedling light responses by inhibiting four negatively-acting phytochrome-interacting factors. *Proc Natl Acad Sci USA* **106**: 7660–7665
- Simpson K, Cerda A, Stange C** (2016a) Carotenoid biosynthesis in *Daucus carota*. *Subcell Biochem* **79**: 199–217
- Simpson K, Fuentes P, Quiroz-Iturra LF, Flores-Ortiz C, Contreras R, Handford M, Stange C** (2018) Unraveling the induction of phytoene synthase 2 expression by salt stress and abscisic acid in *Daucus carota*. *J Exp Bot* **69**: 4113–4126
- Simpson K, Quiroz LF, Rodríguez-Concepción M, Stange CR** (2016b) Differential contribution of the first two enzymes of the MEP pathway to the supply of metabolic precursors for carotenoid and chlorophyll biosynthesis in carrot (*Daucus carota*). *Front Plant Sci* **7**: 1344

- Stange C, Flores C** (2012) Carotenoids and photosynthesis-regulation of carotenoid biosynthesis by photoreceptors. In M Mahadi, ed, *Advances in Photosynthesis: Fundamental Aspects*, Vol. 4. InTech, Rijekia, Croatia, pp 77–96
- Stange C, Fuentes P, Handford M, Pizarro L** (2008) *Daucus carota* as a novel model to evaluate the effect of light on carotenogenic gene expression. *Biol Res* **41**: 289–301
- Stanley L, Yuan YW** (2019) Transcriptional regulation of carotenoid biosynthesis in plants: so many regulators, so little consensus. *Front Plant Sci* **10**: 1–17
- Suslow TV, Wu J, Peiser G** (1999) Characterization of carotenoid composition of carrots affected by 'light root syndrome'. *Integrated View of Fruit and Vegetable Quality*. CRC Press, Boca Raton, FL doi:10.1201/9781351073769.
- Toledo-Ortiz G, Huq E, Rodríguez-Concepción M** (2010) Direct regulation of phytoene synthase gene expression and carotenoid biosynthesis by phytochrome-interacting factors. *Proc Natl Acad Sci USA* **107**: 11626–11631
- Tripathi S, Hoang QTN, Han YJ, Kim J** (2019) Regulation of photomorphogenic development by plant phytochromes. *Int J Mol Sci* **20**: 6165
- Von Lintig J, Welsch R, Bonk M, Giuliano G, Batschauer A, Kleinig H** (1997) Light-dependent regulation of carotenoid biosynthesis occurs at the level of phytoene synthase expression and is mediated by phytochrome in *Sinapis alba* and *Arabidopsis thaliana* seedlings. *Plant J* **12**: 625–634
- Woitsch S, Römer S** (2003) Expression of xanthophyll biosynthetic genes during light-dependent chloroplast differentiation. *Plant Physiol* **132**: 1508–1517
- Zhang X, Henriques R, Lin SS, Niu QW, Chua NH** (2006) Agrobacterium-mediated transformation of *Arabidopsis thaliana* using the floral dip method. *Nat Protoc* **1**: 641–646
- Zhou P, Song M, Yang Q, Su L, Hou P, Guo L, Zheng X, Xi Y, Meng F, Xiao Y, et al.** (2014) Both PHYTOCHROME RAPIDLY REGULATED1 (PAR1) and PAR2 promote seedling photomorphogenesis in multiple light signaling pathways. *Plant Physiol* **164**: 841–852